# Measurements of Three-Dimensional Velocities of Spray Droplets Using the Holographic Velocimetry System

**Yeon-Jun Choo, Bo-Seon Kang***
*Department of Mechanical Engineering, Chonnam National University, 300, Yongbong-Dong, Buk-Gu, Kwangju 500-757, Korea*

The Holographic Particle Velocimetry system can be a promising optical tool for the measurements of three dimensional particle velocities. In this study, the holographic particle velocimetry system was used to measure the sizes and velocities of droplets produced by a commercial full cone spray nozzle. As a preliminary validation experiment, the velocities of glass beads on a rotating disk were measured with uncertainty analysis to identify the sources of all relevant errors and to evaluate their magnitude. The error of the particle velocity measured by the holographic method was 0.75 m/s, which was 4.5% of the known velocity estimated by the rotating speed of disk. The spray droplet velocities ranged from 10.3 to 13.3 m/s with average uncertainty of ±1.6 m/s, which was ±14% of the mean droplet velocity. Compared with relatively small uncertainty of velocity components in the normal direction to the optical axis, uncertainty of the optical axis component was very high. This is due to the long depth of field of droplet images in the optical axis, which is inherent feature of holographic system using forward-scattering object wave of particles.

**Key Words :** Holographic Particle Velocimetry, Spray Droplets, Uncertainty Analysis

## Nomenclature

$d$ : Droplet diameter
$D$ : Distance
$F$ : Conversion factor
$N$ : Number of pixels
$R$ : Radius of disk
$S$ : Size of glass beads
$S_{\bar{x}}$ : Standard deviation of the means
$t_{\nu,P}$ : $t$ estimator with $P\%$ probability and degree of freedom, $\nu$
$\Delta t$ : Laser pulse interval
$u$ : Uncertainty
$u_0$ : Zero-order uncertainty of instrument
$V$ : Velocity of particle
$x$, $y$ : $x$ and $y$ axis
$z$ : $z$ axis (optical axis)

**Greek Symbols**

$\beta$ : Coefficient of system-dependent sensitivity
$\delta$ : Depth of field
$\omega$ : Rotation speed of disk
$\Omega$ : Effective aperture forming the holographic image

**Subscripts**

$a$ : Actual velocity
$m$ : Holographically measured velocity

* Corresponding Author,
**E-mail** : bskang@chonnam.ac.kr
**TEL** : +82-62-530-1683; **FAX** : +82-62-530-1689
Department of Mechanical Engineering, Chonnam National University, 300, Yongbong-Dong, Buk-Gu, Kwangju 500-757, Korea. (Manuscript **Received** December 23, 2002; **Revised** April 21, 2003)

## 1. Introduction

The flow fields encountered in many engineering areas have many complexities and irregularities, as well as being three dimensional in nature. To investigate the characteristics of such flow fields, various measurement techniques and instruments have been developed and commercialized. Among these, non-intrusive optical instruments, such as LDV (Laser Doppler Velocimetry) and PIV (Particle Image Velocimetry)

have advanced remarkably owing to the rapid development of lasers, imaging systems, and computers. However, a measurement tool with the capability of measuring 3-D velocities over a complete test volume as a function of time remains a dream of engineers. In recent years, the focus of research on flow field measurement tools has concentrated on three dimensional velocity measurements. Even though the extension of 2-D PIV to 3-D seems to be a reasonable choice from a short-term standpoint, a holographic method might be an ultimate solution, because of its superiority in the realization of 3-D fields. However, many problems must be overcome because the holographic system remains very much at laboratory-development status level.

As for the spray diagnostic systems, considerable progress in laser instruments like PDPA (Phase Doppler Particle Analyzer) now make it possible to obtain reliable data upon droplet sizes and velocities in dilute sprays. However, they are inherently limited in dense spray regions, where liquid elements are rather large and non-spherical. In addition, no information on the spray structure can be provided by this kind of laser instrument. On the other hand, the holographic technique re-produces the frozen spray as a 3-D image, from which sizes and 3-D velocities of droplets and the spray structure can be investigated.

The holographic technique has been widely used in research on particle sizing for some time (Vikram, 1979). Recently, interest in the use of holography as a tool for 3-D particle velocity determination have increased, to make full use of the 3-D characteristics of holography. The holographic particle velocimetry systems reported to date can be classified into two categories; 1) Direct measurements of sizes and displacements from particle images (Feldmann, 1999; Haussmann and Lauterborn, 1980; Kang, 1995; Lauterborn and Hentschel, 1986; Prikryl and Vest, 1982; Staselko and Kosnikovskii, 1973; Witherow, 1979) and 2) Holographic PIV, which extends the correlation technique used in 2-D PIV to three dimensions (Barnhart and Adrian, 1994; Meng and Hussain, 1995; Zhang et al., 1997; Zimin et al., 1993).

As examples of the former method, Feldmann (1999) obtained the 3-D displacements of moving bubbles by recording two-side holograms of bubbles and matching bubbles in both directions. Kang (1995) used a two-reference-beam double-pulse technique, which featured switching the polarization of the laser light between pulses to separate the first and second droplet images. This avoided the overlapping problem or the directional ambiguity of particle movement. The method developed by Kang (1995) was applied to fan-shaped sprays formed by two impinging high-speed jets.

As for the latter method, Barnhart and Adrian (1994) also used two reference beams to record the separate image of particles, and then they adopted a stereoscopic PIV technique to obtain 3-D turbulent flow fields. Zhang et al. (1997) developed the hybrid HPIV system, which adopted the advantages of in-line and off-axis holography, and Meng et al. (1993, 1995) conducted several significant studies on HPIV, and introduced the IROV (in-line recording and off-axis viewing) system (Meng and Hussain, 1995), a multibeam technique (Zimin et al., 1993).

This paper reports the results of a preliminary study at the intermediate stage of the development of the holographic velocimetry system for spray droplets. The ultimate objective of research is to develop a holographic velocimetry system to automatically measure the sizes and the 3-D velocities of droplets using a particle tracking method. As a preliminary step, validation experiments were conducted to compare the holographic measurement results of the sizes and velocities of glass beads on a rotating disk with known values. Uncertainty analysis was performed to identify the sources of relevant errors in the measurements of displacement, size, and the velocities of particles and to evaluate their magnitudes. Finally, the sizes and 3-D velocities of spray droplets were measured by the manual image processing based on the operator's judgment. These measurement results may provide important information for the development of the holographic velocimetry system based on the automatic image processing.

## 2. Experimental Apparatus and Methodology

### 2.1 Holographic recording system

Figure 1 shows a schematic layout of the holographic recording system used in this study. The light source for the fabrication of pulsed holograms was a twin Nd-YAG laser (Brilliant B, Quantel), which generated wavelength of 532 nm, vertically polarized, and 300 mJ output energy laser beams of frequency 10 Hz. An injection-seeder was used to increase the coherence length of the output laser to more than one meter for holographic application. The pulse interval between the two lasers was controllable from 1 to 900 $\mu$s. The short pulse duration (10 ns) used assured the freezing of all moving particles and the clarity of the resulting images.

The light from the laser was separated using a beamsplitter, which divided the beam into reference and object beams. The object beam was expanded and collimated to a diameter of 10 cm using a Galilean type of beam expander for the high power pulsed laser. This plane wave was passed through the test section and finally was intercepted at the $10.16 \times 12.7$ cm holographic glass plate. The beam intensity was adjusted by an attenuator to achieve a reference-to-object beam intensity ratio of approximately 4 to 1, which was selected by trial-and-error. The reference beam was at an angle of 28° relative to the normal of the holographic plate. A diffuser was positioned before the test section to provide a uniform background and to decrease the depth of field of the particle image. The difference of path lengths between the object and reference beams was minimized to guarantee satisfactory interference between both beams irrespective of the coherence length of the laser.

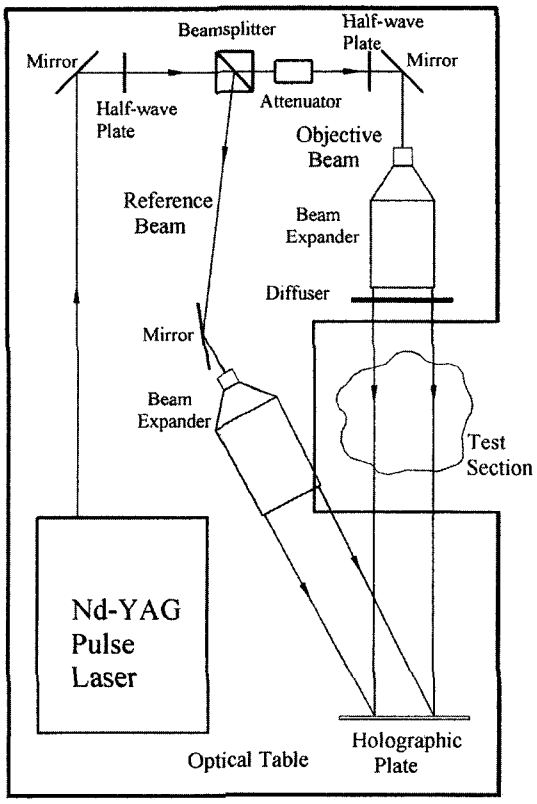


**Fig. 1** Schematic diagram of the holographic recording system

### 2.2 Measured particle systems

Once the holographic particle velocimetry system has been developed, results obtained on particle velocities should be verified against some kind of experimental system, in which the particle velocities are already known and easily changed. For this purpose, small glass beads on a rotating disk were used, as shown schematically in Fig. 2. The system consists of a driving motor and a horizontally positioned rotating disk of diameter 300 mm on which glass beads of several millimeters in diameter were attached to the tips of thin wires of different lengths. Six glass beads of similar size were located at each radius of 85,

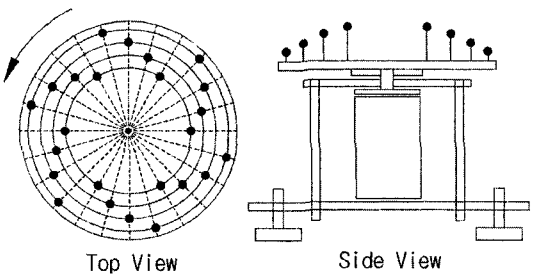


**Fig. 2** Experimental apparatus of the rotating disk system apparatus

105, 115, and 125 mm. The rotating speed was controllable to 3,000 rpm using a DC power controller. The possible maximum velocity of glass beads located at periphery of the disk was 40 m/s at the highest rotating speed of the disk.

After validation experiments, the sizes and velocities of real spray droplets were measured. A high-pressure $N_2$ gas cylinder with a pressure regulator was used to pressurize a liquid reservoir to direct non-fluctuating stable liquid to flow to a commercial spray nozzle (full cone type, Spraying Systems Co.). Water was injected with injection pressure of 245 kPa through the 1.0 mm nozzle hole.

### 2.3 Hologram reconstruction and image processing system

The recorded holograms were developed, fixed, and dried as for photographic film processing, and then reconstructed and analyzed using an image processing system as shown in Fig. 3. The laser used in the reconstruction of the holograms was a diode-pumped crystal laser of the same wavelength for recording (532 nm). Real particle images were captured rather than virtual images to obtain the maximum allowable magnification of particle images by close-up. The digital CCD camera (Kodak Co., 1,024×1,024 pixels) was moved automatically using a three axes translation stage (PI) and positioned with a resolution of 30 $\mu$s. The measurements of sizes and moving distances of particles from captured particle images were performed manually using image processing software (Inspector, Matrox Inc.).

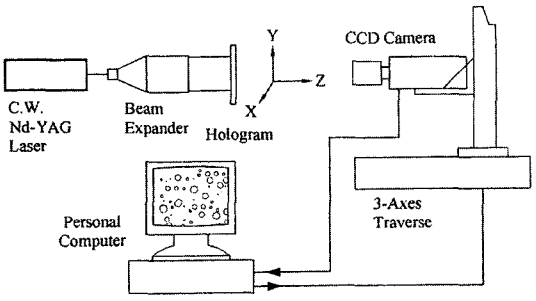


**Fig. 3** Image reconstruction and processing system

## 3. Experimental Results and Discussion

### 3.1 Validation experiments

To verify the velocity measurements made using the holographic method, double pulse images of glass beads located at a radius of 125 mm at a rotation speed of 813 or 1,284 rpm, and a pulse interval of 500 $\mu$s were captured and analyzed. Figure 4 shows holographically reconstructed double pulse image of particles. The left and right particles in each figure were recorded at the first and second pulses and Fig. 4(a) focused on the left particle and Fig. 4(b) on the right particle.

The actual velocity of a particle is

$$V_a = R \times \omega \tag{1}$$

The uncertainty of measurement in the actual velocity of the particle, $v_{V,a}$, can be expressed as follows by the propagation of uncertainty (Figliola and Beasley, 1998).

$$u_{V,a} = \sqrt{\left(\frac{\partial V_a}{\partial R} u_R\right)^2 + \left(\frac{\partial V_a}{\partial \omega} u_\omega\right)^2} = \sqrt{(\omega u_R)^2 + (R u_\omega)^2} \tag{2}$$

Here, $u_R$ is the uncertainty in the radius measurement by Vernier caliper and this is ±0.025 mm. The uncertainty of the rotation speed of the disk $u_\omega$, consists of the zero-order uncertainty of the instrument (±0.5 rpm) and the precision error associated with multiple measurements.

$$u_\omega = \sqrt{(u_0)^2 + (t_{\nu,P} S_{\bar{x}})^2} \tag{3}$$

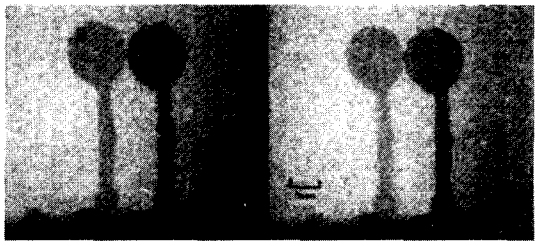

(a) (b)

**Fig. 4** Holographically reconstructed double image of particle; particle image of (a) first pulse (b) second pulse is focused

Particle velocities by the holographic technique are obtained by dividing the distance moved by the particles by the pulse interval. The measurable maximum particle velocity can be approximately estimated $10^4$ m/s by using the lowest pulse duration (1 $\mu$s) and the allowable maximum moving distance (1 cm). More details about uncertainty analysis on the holographic technique can be found in our previous work (Oh et al., 2002) and some related contents required for the measurements of droplet velocities are explained here.

The conversion factor, $F$, which relates the actual distance per one pixel of images, was obtained by using the hologram of a 5 mm scale. It was 0.04464 mm/pixel with 112 pixels representing a 5 mm scale and the uncertainty in the conversion factor, $u_F$, was $\pm$0.001197 mm/pixel.

The distances moved by particles in the $x$ and $y$ directions were obtained by multiplying the number of pixels between the centers of particles at each pulse by the conversion factor. Therefore, the uncertainty of distance measurement in the $x$ and $y$ directions can be expressed as

$$u_{Di}=\sqrt{\left(\frac{\partial D_i}{\partial F}u_F\right)^2+\left(\frac{\partial D_i}{\partial N}u_N\right)^2} =\sqrt{(Nu_F)^2+(Fu_N)^2} \quad (1)$$

The uncertainty in the number of pixels, $u_N$, was assumed to be $\pm$2 pixels.

One of inherent characteristics of particle holography using forward scattered light by particles is the very long depth of field of particle images in the optical axis compared with the very short depth of a normal camera. This characteristic causes considerable difficulty in the determination of particle positions in the optical axis. In the present study, several seemingly in-focus particle images were captured first by moving a CCD camera along the optical axis, and then the depth was determined by using the change in the gradient of gray values of particles and background or by the operator. The particle position in the $z$ direction was determined as the center of this depth. As for the uncertainty of distance measurement in the $z$ direction, $u_{D_z}$, the depths for one particle for the cases of 813 and 1,284 rpm, were $\pm$0.06 and 0.07 mm, respectively. Therefore, $u_{D_z}$ was assumed to be twice these values, that is, $u_{D_z}=\pm$0.12 and 0.14 mm.

The components of particle velocity in each direction are calculated by division of moved distances by the pulse interval so the uncertainty of particle velocity in each direction is expressed as

$$u_{V_i}=\sqrt{\left(\frac{\partial V_i}{\partial D_i}u_{D_i}\right)^2+\left(\frac{\partial V_i}{\partial \Delta t}u_{\Delta t}\right)^2} =\sqrt{\left(\frac{1}{\Delta t}u_{D_i}\right)^2+\left(\frac{D_i}{\Delta t^2}u_{\Delta t}\right)^2} \quad (5)$$

The uncertainty of laser pulse interval, $u_{\Delta t}$, is zero. The magnitude of particle velocity is obtained from the components of velocity and the uncertainty of the particle velocity measured by the holographic method, $u_{V,m}$, is calculated from

$$u_{V,m}=\sqrt{\left(\frac{\partial V}{\partial V_x}u_{V_x}\right)^2+\left(\frac{\partial V}{\partial V_y}u_{V_y}\right)^2+\left(\frac{\partial V}{\partial V_z}u_{V_z}\right)^2} \quad (6)$$

Based on above analysis, the actual and measured velocities of the glass beads with their uncertainties and the relative errors of measurements are summarized in Table 1. Here, $V_x$ and $V_z$ are velocity components in the $x$ and $z$ axis and $V_m$ is the magnitude of the particle velocity. The values in parenthesis represent the uncertainty expressed as a percentage of the measured value.

**Table 1** Comparison of actual glass bead velocities with measured values

| Actual Velocity (m/s) | | Measured Velocity (m/s) | | | Error (m/s) |
|---|---|---|---|---|---|
| RPM | $V_a$ | $V_x$ | $V_z$ | $V_m$ | |
| 813± 2.05 (0.3%) | 10.637± 0.027 (0.3%) | 5.850± 0.165 (2.8%) | 8.550± 0.224 (2.6%) | 10.365± 0.207 (2.0%) | 0.272 (2.6%) |
| 1284± 1.37 (0.1%) | 16.799± 0.020 (2.8 %) | 8.316± 0.280 (3.4 %) | 13.722± 0.285 (2.1%) | 16.045± 0.284 (1.8%) | 0.754 (4.5%) |

The greatest error of the particle velocity measured by the holographic technique is 0.75 m/s, which is 4.5% of the actual velocity. The greatest uncertainty of the holographic measurements was 0.28 m/s, which is ±3.4% of the measured value.

### 3.2 Droplet size and velocity measurements

The velocities of spray droplets and uncertainties in the measurements are obtained as in the same method described in the validation experiments except for uncertainty in the direction, because spray droplets are much smaller than the glass beads. As explained above, the uncertainty in the determination of particle positions in the $z$ direction is related with to the depth of field of the particle. The depth of field is defined as the maximum defocusing distance from the exact image position that does not cause a significant change in the particle image. According to the Meng and Hussain's analysis (1995) for particles recorded and reconstructed by using the holographic system, the depth of field, $\delta$, depends on the size of the particles and the optical system used.

$$\delta=\beta\frac{d}{\Omega} \tag{7}$$

Here, $\beta$ is a coefficient introduced to incorporate the system-dependent sensitivity and $\Omega$ is the effective aperture forming the holographic image.

Based on above analysis, the particle diameter was selected as a parameter for the uncertainty in the determination of a particle's positions in the $z$ direction. The next problem is what fraction of diameter can be considered as the uncertainty. To determine this, the focal plane of a camera was gradually moved from the focused position of droplet. Figure 5 shows the difference in droplet images due to the movement of the focal plane. Defocusing gradually became severe as the focal plane was moved over 0.5 $d$ from the focused plane. Therefore, 0.5 $d$ was selected as the uncertainty in the determination of a particle's positions in the $z$ direction. Two particles were involved in the measurement of the distance moved in the $z$ direction resulting in $u_{D_z}=\pm d$ mm. As this method is less than satisfactory and it results in large uncertainty in the optical axis compared with the other axes, supplementary experiments using orthogonal two-side holography are underway to more accurately evaluate the magnitude of the uncertainty in the determination of a particle's positions along the optical axis. Even though this problem may be solved, the application of this technique to the dense region of spray may be limited due to the relatively long depth of focus of particles.

Figure 6 shows the typical double pulse image of spray droplets, which were holographically recorded with a pulse interval of 100 $\mu$s and then reconstructed. The measurement results of sizes

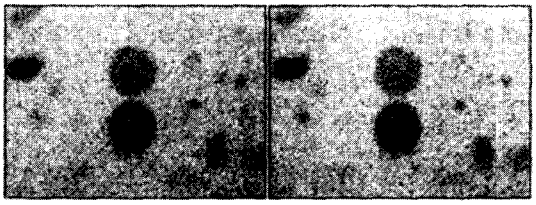

(a) Focused droplet (b) 0.5 $d$

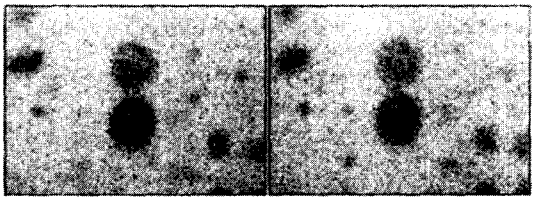

(c) 1.5 $d$ (d) 3.0 $d$

**Fig. 5** Differences in focused droplet image due to the focal plane movement

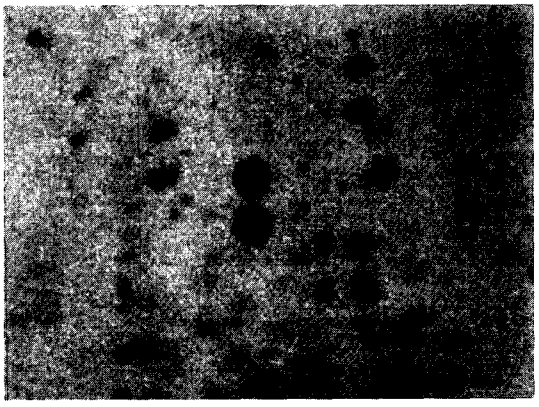

**Fig. 6** Holographically reconstructed double pulse image of spray droplets

**Table 2** Results of droplet velocity and diameter measurements

| No. | Position (mm) | | | Velocity (m/s) | | | V (m/s) | Diameter ($\mu$m) |
|---|---|---|---|---|---|---|---|---|
| | $x$ | $y$ | $z$ | $V_x$ | $V_y$ | $V_z$ | | |
| 1 | −1.35 | 5.92 | 15.73 | −2.90±0.39 | 10.93±0.71 | 6.99±4.76 | 13.29±2.25 | 476±24 |
| 2 | −4.25 | 10.33 | −2.00 | −3.02±0.54 | 10.71±0.67 | −2.33±2.99 | 11.37±0.89 | 299±15 |
| 3 | −11.52 | 16.48 | −0.73 | −4.42±0.43 | 9.17±0.58 | −1.99±1.33 | 10.37±0.60 | 133±7 |
| 4 | −6.92 | 20.22 | 5.00 | −5.14±0.46 | 9.87±0.62 | 3.33±3.38 | 11.62±1.13 | 338±17 |
| 5 | −4.12 | 27.74 | −16.67 | −0.79±0.31 | 10.15±0.64 | −2.33±3.30 | 10.45±0.97 | 331±17 |
| 6 | 8.83 | 38.33 | 26.33 | 1.39±0.35 | 10.46±0.67 | 4.67±4.56 | 11.55±1.94 | 457±24 |
| 7 | −10.14 | 45.59 | −11.89 | −1.55±0.30 | 9.38±0.60 | −5.53±3.53 | 10.99±1.85 | 353±18 |
| 8 | −18.13 | 48.82 | −17.33 | −1.87±0.32 | 9.17±0.58 | −6.67±4.36 | 11.98±2.48 | 437±22 |
| 9 | 4.32 | 54.02 | −27.67 | 1.55±0.37 | 9.86±0.62 | −6.67±2.53 | 12.01±1.49 | 253±13 |
| 10 | 17.32 | 58.12 | 11.40 | 3.89±0.56 | 10.65±0.71 | 0.82±4.26 | 11.33±0.75 | 426±22 |
| 11 | −4.75 | 60.22 | 26.70 | −0.50±0.41 | 9.97±0.63 | 4.00±5.06 | 12.49±1.76 | 506±26 |
| 12 | −13.25 | 67.12 | 21.40 | −1.95±0.34 | 9.97±0.63 | 3.33±3.73 | 10.69±1.30 | 373±19 |
| 13 | −12.51 | 73.21 | 25.60 | −1.47±0.28 | 10.66±0.62 | 4.67±3.33 | 11.73±1.44 | 333±17 |
| 14 | 1.09 | 74.21 | 26.00 | 0.53±0.37 | 9.03±0.65 | 8.80±3.99 | 12.62±2.83 | 399±20 |
| 15 | 15.21 | 74.93 | 4.00 | 1.85±0.35 | 10.05±0.58 | 1.22±2.95 | 10.29±0.67 | 295±15 |
| 16 | 9.15 | 75.56 | −5.00 | 0.88±0.38 | 10.29±0.55 | −6.67±5.80 | 12.29±3.28 | 581±30 |
| 17 | 14.50 | 78.52 | 14.53 | 1.79±0.29 | 11.68±0.67 | 3.99±4.38 | 12.48±1.54 | 439±23 |

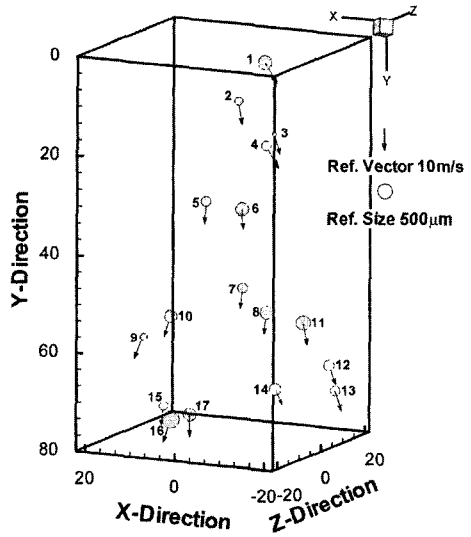


**Fig. 7** Positions, sizes, and velocities of measured droplets

and 3-D velocities of droplets are summarized in Table 2 and schematically shown in Fig. 7, with the nozzle exit taken as an origin of axes. Each component and magnitude of droplet velocity is shown in Fig. 8 and Fig. 9, respectively, with error bars representing the uncertainties shown in Table 2.

As shown in Fig. 6, the components of droplet velocities show the expected behavior of droplet movements, which is radially outward and axially downward. The highest component of droplet velocities occurs in the $y$ direction, namely, in the axis of the spray. These velocities range from 9.0 to 11.7 m/s with an average velocity of 10.3 m/s. The average of the corresponding uncertainties is ±0.64 m/s, which is ±6% of the average velocity. The velocity component in the $x$ and $z$ directions are lower than in the $y$ direction. The velocity component in the $x$ direction varies from 0.5 to 5.1 m/s with average velocity of 2.1 m/s. The average uncertainty is ±0.4 m/s, which is ±18% of the average velocity. The uncertainties of velocity components in the $x$ and $y$ directions, which are the normal directions to the optical axis, are under ±0.7 m/s and this value is not high compared with the magnitude of the droplet velocity. On the other hand, the velocity component in the $z$ direction changes from 0.8 to 8.8 m/s with average velocity of

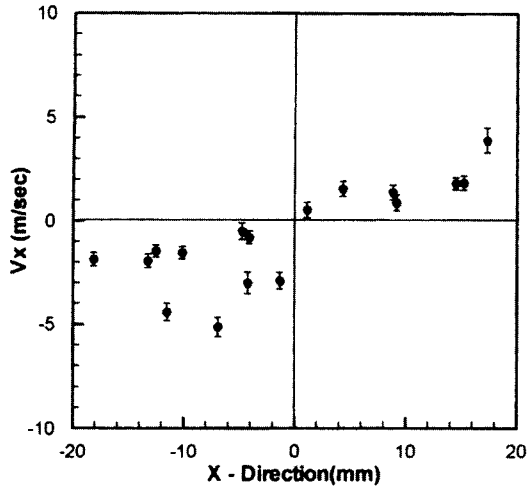


(a) $x$-axis velocity

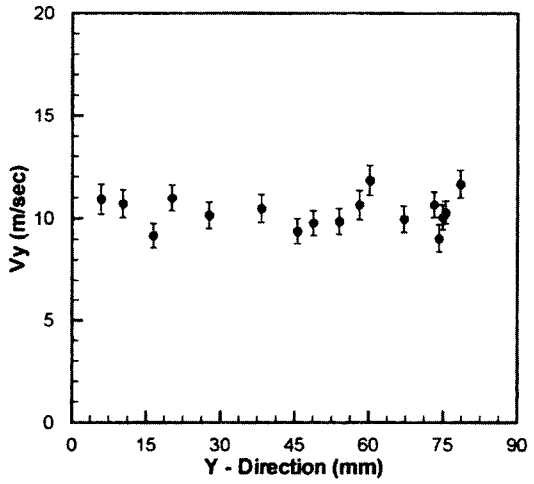


(b) $y$-axis velocity

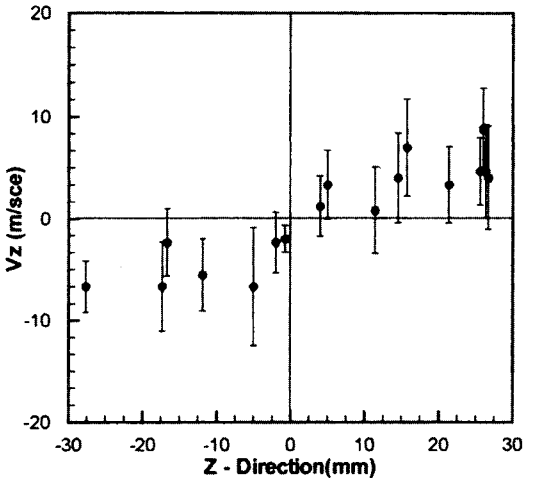


(c) $z$-axis velocity

**Fig. 8** Velocity components of droplets

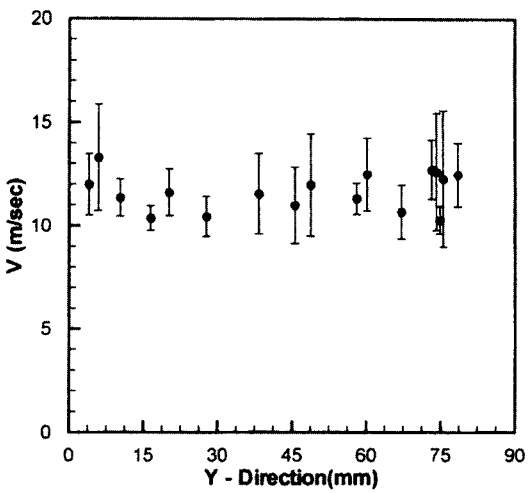


**Fig. 9** Magnitude of droplet velocities

4.4 m/s. The average uncertainty is $\pm 3.4$ m/s, which is very high compared with the relatively small uncertainties of the velocity components in directions normal to the optical axis. As explained before, this is due to the long depth of field of the droplet images in the optical axis, which is an inherent feature of the holographic system using forward-scattering object wave of particles.

The magnitude of the droplet velocities ranges from 10.3 to 13.3 m/s with average value of 11.6 m/s and the average of uncertainty is $\pm 1.6$ m/s, which is $\pm 14\%$ of the average velocity. The relatively large uncertainties resulted from the large uncertainties in the optical axis and supplementary experiments are underway to improve the uncertainty in the optical axis.

The sizes of droplets are obtained by evaluating the equivalent diameter of droplets from the total area of droplet images. The measured diameters of droplets are also shown in Table 2. The sizes range from 133 to 581 $\mu$m with an average diameter of 378 $\mu$m. The average uncertainty of size measurements is $\pm 20$ $\mu$m, which is $\pm 5\%$ of average diameter.

## 4. Conclusion

In this study, the sizes and velocities of droplets produced by a commercial full cone spray nozzle

were measured using the holographic velocimetry system with manual image processing. As a validation experiment, the velocities of glass beads on a rotating disk were measured using the double pulse holographic system and the measurement results were compared with the known velocities obtained from the rotating speed of the disk. Uncertainty analysis in the measurements of particle velocities by the holographic method was performed to identify the sources of all relevant errors and to evaluate their magnitudes.

The measurement results of velocities obtained with the holographic method were compared reasonably well with the know values, within acceptable error ranges. To be specific, the error of the glass bead velocity measured by the holographic method was 0.75 m/s, which was 4.5% of the known velocity as estimated by the rotating speed of the disk. The uncertainty of the holographic measurements was $\pm 0.28$ m/s, which was $\pm 3.4\%$ of the measured value. The spray droplet velocities ranged from 10.3 to 13.3 m/s with an average uncertainty of $\pm 1.6$ m/s, which was $\pm 14\%$ of the mean droplet velocity. Compared with relatively small uncertainty in velocity components in the directions normal to the optical axis, that of the optical axis component is $\pm$ 3.6 m/s. This large uncertainty is attributed to the long depth of droplet image in the optical axis, which is an inherent feature of a holographic system using forward-scattering objects wave of particles.

## Acknowledgment

This work was supported by a grant No. R05-2000-000-00297-0 from Korea Science and Engineering Foundation.

## References

Barnhart, D. H. and Adrian, R. J., 1994, "Phase-Conjugate Holographic System for High-Resolution Particle-Image Velocimetry," *Applied Optics*, Vol. 33, pp. 7159~7170.

Feldmann, O., 1999, "Short-Time Holography and Holographic PIV Applied to Engineering Problems," *Applied Optical Measurements*, Springer-Verlag.

Figliola, R. S. and Beasley, D. E., 1998, *Theory and Design for Mechanical Measurement*, John Wiley & Sons, pp. 181~232.

Haussmann, G. and Lauterborn, W., 1980, "Determination of Size and Position of Fast Moving Gas Bubbles in Liquids by Digital 3-D Image Processing of Hologram Reconstruction," *Applied optics*, Vol. 19, No. 20, pp. 3529~3535.

Kang, B. S., 1995, "A Holographic Study of The Dense Region of a Spray Created by Two Impinging Jets," Ph. D. Thesis, Univ. of Illinos at Chicago.

Lauterborn, W. and Hentschel, W., 1986, "Cavitation Bubble Dynamics Studied by High Speed Photography and Holography : Part Two," *Ultrasonics*, Vol. 24, No. 2, pp. 59~65.

Meng, H. and Hussain, F., 1995, "In-Line Recording and Off-Axis Viewing Technique for Holographic Particle Velocimetry," Applied Optics, Vol. 34, pp. 1827~1840.

Oh, D. J., Choo, Y. J., and Kang, B. S., 2002, "Experimental Validation for the Development of Holographic Particle Velocimetry System for Spray Droplets," *Transactions of the KSME*, Vol. 26, No. 4, pp. 539~546 (in Korea).

Prikryl, I. and Vest, C. M., 1982, "Holographic Imaging of Semitransparent Droplets," *Applied Optics*, Vol. 21, No. 14, pp. 2541~2547.

Staselko, D. I. and Kosnikovskii, V. A., 1973, "Holographic Recording of Three-Dimensional Ensembles of Fast-Moving Particles," *Optics and Spectroscopy*, Vol. 34, No. 2, pp. 206~210.

Vikram, C. S., 1979, *Particle Field Holography*, Cambridge University Press.

Witherow, W. K., 1979, "A High Resolution Holographic Particle Sizing System," *Optical Engineering*, Vol. 18, No. 3, pp. 249~255.

Zhang, J., Tao, B. and Katz, J., 1997, "Turbulent Flow Measurement in a Square Duct with Hybrid Holographic PIV," *Experiments in Fluids*, Vol. 23, pp. 373~381.

Zimin, V., Meng, H. and Hussain, F., 1993, "Innovative Holographic Particle Velocimeter ; A Multibeam Technique," *Optical Letters*, Vol. 18, No. 13, pp. 1101~1103.